

Synthesis and characterization of Hf_2PbC , Zr_2PbC and M_2SnC ($\text{M} = \text{Ti}, \text{Hf}, \text{Nb}$ or Zr)

T. El-Raghy, S. Chakraborty, M.W. Barsoum*

Department of Materials Engineering, Drexel University, 32nd and Chestnut Street, Philadelphia, PA 19104, USA

Received 6 January 2000; received in revised form 28 March 2000; accepted 11 April 2000

Abstract

Predominantly single phase (92–94 vol. %), fully dense samples of Hf_2SnC , Zr_2SnC , Nb_2SnC , Ti_2SnC , Hf_2PbC and Zr_2PbC were fabricated by reactively HIPing the stoichiometric mixture of the corresponding elemental powders in the 1200–1325 °C temperature range for 4–48 h. The latter two, fabricated here for the first time, required a further anneal of 48–96 h to increase the volume fraction of ternary phases. Hf_2PbC and Zr_2PbC are unstable in ambient atmospheres at room temperature. As a family these compounds are good electrical conductors; the lowest and highest values of the electrical conductivities were, respectively, $2.2 \times 10^6 (\Omega \cdot \text{m})^{-1}$ for Hf_2SnC and $13.4 \times 10^6 (\Omega \cdot \text{m})^{-1}$ for Hf_2PbC . The Vickers hardness values range from 3 to 4 GPa. All compounds are readily machinable. The Young's moduli of Zr_2SnC , Nb_2SnC and Hf_2SnC are, respectively, 178, 216 and 237 GPa. The thermal coefficients of expansion, TCE's, of the ternaries scale with those of the corresponding binaries, and are relatively low for such readily machinable solids. The lowest TCE belonged to Nb_2SnC [$(7.8 \pm 0.2) \times 10^{-6} \text{ K}^{-1}$], and the highest to Ti_2SnC [$(10 \pm 0.2) \times 10^{-6} \text{ K}^{-1}$]. The TCE's of Hf and Zr containing ternaries cluster around $(8.2 \pm 0.2) \times 10^{-6} \text{ K}^{-1}$. All the synthesized ternary carbides were found to dissociate into the transition metal carbide and the A-group element in the 1250–1390 °C temperature range. © 2000 Elsevier Science Ltd. All rights reserved.

Keywords: Carbides; Elastic modulus; Electrical conductivity; Hardness; Hot isostatic pressing; Thermal expansion

1. Introduction

The ternary compounds with the general formula $\text{M}_{n+1}\text{AX}_n$, where $n = 1-3$, M is an early transition metal, A is an A-group (mostly IIIA and IVA) element and X is either C and/or N, are structurally related.¹⁻⁶ In these compounds, near close-packed transition metal carbide and/or nitride layers are interleaved with layers of pure A-group element. In the M_2AX , or 211's¹⁻³ phases every third layer is an A layer; in the M_3AX_2 , or 312's,^{3,4} every fourth layer, and in the M_4AX_3 , or 413's, every fifth layer.^{5,6} By now it is fairly well established that as a class, these ternaries possess an unusual set of properties: they are machinable, good thermal and electrical conductors, anomalously soft (Vickers hardness 2–4 GPa), thermal shock resistant and damage tolerant, elastically stiff, have relatively low thermal expansion coefficients ($< 10 \times 10^{-6} \text{ }^\circ\text{C}^{-1}$) and combine mechanical anisotropy with thermal isotropy.⁷⁻²² This combination of properties derives

partially from the metallic nature of the bonding and partially from the layered nature of the structure. We have also shown that, at least in Ti_3SiC_2 , basal slip is operative at room temperature¹⁵ and that deformation occurs by a unique combination of kink and shear band formation.^{16,17}

This work deals with the Sn and Pb containing 211 phases, namely: M_2SnC where M is Ti, Hf, Zr or Nb, and M_2PbC , where M is either Hf or Zr. In the original work by Jeitschko and co-workers, these ternary carbides were synthesized by sealing mixed elemental powders in the appropriate molar ratios in evacuated quartz tubes and annealing them at 800 °C for several hundreds of hours.^{1,2} The samples were powdered, X-rayed and their lattice parameters were calculated. In 1997 Barsoum et al.¹⁰ synthesized the Sn-containing phases in fully dense bulk form by reactively hot isostatic pressing (HIPing) elemental powders at $T > 1200^\circ\text{C}$ and for shorter annealing times as compared to the original work.^{1,2} Preliminary measurements included Vickers hardness, electrical conductivities and their temperature dependencies.¹⁰

Another distinguishing feature of these ternaries is their dissociation behavior; instead of melting congruently they

* Corresponding author. Tel.: +1-215-895-2338; fax: +1-215-815-6760.

E-mail address: barsoumw@drexel.edu (M.W. Barsoum).

Table 1
Sources and characteristics of powders used

Powder	Purity	Particle size	Source
Ti	99.0%	–325 mesh	Johnson Matthey, MA
Hf	99.6% (Zr nominal 2–3.5%)	–325 mesh	Alfa Aesar, Ward Hill, MA
Zr	99.8%	–325 mesh	Prochem Inc., Rockford, Ill.
Nb	99.0%	–325 mesh	Alfa Aesar, Ward Hill, MA
Sn	99.8%	–325 mesh	Aldrich Chemicals, Milwaukee, WI
Pb	99%	–325 mesh	Prochem Inc., Rockford, Ill.
Graphite	99.0%	1–2 μm	Aldrich Chemicals, Milwaukee, WI

peritectically decompose into the A-group element and the transition metal carbide, MC_x , at temperatures in excess of 1250°C.^{9,10}

The aim of this work was twofold. The first was to optimize the processing parameters of the M_2SnC phases and further characterize them. The second was to fabricate and characterize, for the first time, predominantly single phase samples of all the currently known Pb-containing ternaries, namely, Ti_2PbC , Hf_2PbC and Zr_2PbC . However, despite our best efforts, and for reasons that are discussed elsewhere,²⁰ we were unable to fabricate Ti_2PbC in pure enough form to characterize it. Furthermore, we discovered that the Pb-containing ternaries were unstable in ambient atmospheres, which limited the scope of their characterization.

2. Experimental details

The starting mixtures consisted of powders of the corresponding transition metal, Sn or Pb and graphite in the 2:1:1 stoichiometry, respectively. The sources of powders for the current work and their purities are listed in Table 1. The powders were ball-milled using Al_2O_3 balls for 24 h to ensure good mixing and to break up any agglomerates. The mixed powders were cold pressed under ~ 280 MPa in 32×13 mm² steel dies. The high green densities (Table 2) are attributed to the deformation of the soft constituents, viz., Sn, Pb and the transition metal.

Green bodies with typical thicknesses of ~ 4 –8 mm were sealed under vacuum in borosilicate (Pyrex) glass tubes. Special care was taken to insure that the thicknesses of the green bodies were at most half the internal diameter of the glass tubes (15 mm). This was necessary because an overall expansion, or swelling, that roughly doubled the size of the green body, during heat up was observed. The reason for this swelling is not clear at this time, but could be related to the de-wetting observed when the melting points of the Pb or Sn were reached. If the size of the samples relative to the tube diameter were too large, the swelling broke the glass tubes during heating, thereby preventing any HIPing action. For the Ti_2SnC samples the maximum thickness of green bodies

successfully HIPed was ≈ 4 mm and these had to be sealed in slightly larger (20 mm) diameter tubes.

All samples were heated at 5°C/min to 850°C, a temperature at which the glass tubes soften. The slow heating rate was found to aid in the re-absorption of the liquid Sn or Pb into the porous preform. Upon reaching 850°C the HIP was pressurized to 55 MPa and heating was resumed at the same heating rate to the processing temperature, at which point the pressure in the HIP increased to 60–70 MPa. The various compositions were held at the processing temperatures for different times varying from 4–48 h (Table 2). Once cooled, the samples were removed from the HIP and the surrounding glass was removed by mechanical grinding using a SiC grinding wheel. The samples were sliced, mounted and polished down to 1 μm using diamond suspension, for optical and scanning electron microscopy, SEM, evaluation. Powders were drilled from the bulk of the samples for X-ray diffraction, XRD characterization. The densities of the HIPed samples were measured using Archimedes' method in water at ambient temperatures.

The most challenging aspect of this work remains determining the optimal processing temperature. The main problem is that too high a temperature results in dissociation, while too low a temperature results in either incomplete reactions, or porous samples. The problem is further complicated by the fact that in most microstructures, the MC_x compound is present and it is nontrivial to determine whether its presence is due to dissociation or insufficient reaction.¹ When the decomposition temperature of the ternary is high, the problem is less severe than when it is low because the HIPing can be carried out at temperatures high enough to result in densification. The problem is more severe when the decomposition temperature is in the vicinity of 1200°C. Thus, in addition to the HIP runs, separate runs, at successively higher temperatures, were carried out to determine the decomposition temperatures of the samples. After each such run the samples were cooled, pulverized and X-rayed.

In all samples, in addition to the MC_x phases, Sn or Pb were detected. The contents of the latter were quantified using a differential scanning calorimeter (DSC)

¹ The MC_x phases form upon heating, i.e. they are in the reaction path.

Table 2
Summary of processing details of, and ancillary phases in, M₂AC compounds fabricated in this work and our previous work

	Ti ₂ SnC	Hf ₂ SnC	Zr ₂ SnC	Nb ₂ SnC	Hf ₂ PbC	Zr ₂ PbC
Green density (g/cm ³)	4.7	8.7	5.5	6.4	9.6	6.8
Relative green density (%)	88.7	87.3	86.8	87.3	85	87.6
Volume change (%) for: 2 M + A + C = M ₂ AC	–17	–15	–12	–13	–6	–15
Processing temperature (°C)	1250	1325	1200	1300	1200	1200
	1325 ¹⁰	1325 ¹⁰	1250 ¹⁰	1300 ¹⁰		
Processing time (h)	12	4	12	4	48 ^a	48 ^b
	4 ¹⁰	4 ¹⁰	4 ¹⁰	4 ¹⁰		
Vol.% Sn or Pb	5.5	1.1	2.3	4.2	2.4	0.4
Vol.% MC _x	< 1	2.5	1.0	3.9	2.0	6.0
Vol.% porosity	< 1	< 1	< 1	< 1	< 1	< 1
Theo. density (g/cm ³)	6.35	11.79	7.16	8.38	12.1	9.2
Calculated density ^c (g/cm ³)	6.38	11.76	7.16	8.31	12.1	9.1
Measured density (g/cm ³)	6.1	11.2	6.9	8.0	11.5	8.2
	6.1 ¹⁰	11.8 ¹⁰	7.0 ¹⁰	8.3 ¹⁰		

^a Followed by a 48 h anneal under Ar at 1200°C.

^b Followed by a 96 h anneal under Ar at 1200°C.

^c Calculated using rule of mixtures and volume fraction listed above.

(Perkin Elmer thermal analysis system). The details can be found elsewhere,²⁰ but entailed comparing the areas under the endothermic peaks due to the melting of the Sn or Pb in the ternary compounds, with the area for a pure sample of known weight. The volume fractions of the MC_x phases were determined by applying an etching solution 1:1:1 by volume of H₂O, HF and HNO₃ to the surface of mounted and polished M₂SnC samples. The solution preferentially attacked the M₂SnC and the Sn in the microstructure leaving the transition metal carbide unaffected. These samples were then evaluated under the optical microscope whereby the carbide regions appear as bright spots, at which point image analysis was used to estimate the MC_x volume fraction.

The elastic constants were measured using a standard pulse-echo method utilizing the heterodyne phase detection (PST) described in detail elsewhere.²¹

The electrical resistances and their temperature dependencies, in the 77–300 K temperature range, were measured with a micro-ohmmeter (Model 5600 AEMC Instruments). The samples were placed in a Dewar flask just above the liquid nitrogen level, the slow evaporation of which allowed for the slow heating of the samples. The temperature was measured by a thermocouple attached directly to the sample. From the results, the temperature coefficients of resistivity, α , was calculated. The latter is defined by:

$$\rho(\mu\Omega.m) = \rho_{300}[1 - \alpha(\Delta T)]$$

where T , ρ and ρ_{300} are, respectively, the temperature in degrees Kelvin, the resistivity at T and at 300 K.

The thermal coefficient of expansion, TCE, was measured under flowing Ar in the 25–1000°C temperature range in a dilatometer (Unitherm, Anter Corp., Pittsburgh, PA). The measurements were carried out both

during the heating and cooling at 2°C/min under Ar. For most samples, there was little hysteresis between the cooling and heating curves and a least squares fit of both curves was used to determine the TCE. The Hf-containing samples, however, showed a marked hysteresis and consequently only the cooling curves were used to calculate their TCE's.

3. Results and discussion

3.1. Processing of M₂SnC compounds

The HIPing temperatures required to produce predominantly single phase samples of the M₂SnC phases are summarized in Table 2, and range from 1200°C for Zr₂SnC, to 1325°C for Hf₂SnC. The times needed to fully densify the samples varied from 4 to 12 h. In general, the lower the processing temperatures the longer the times needed for densification. The porosity in all samples was measured, using image analysis, to be < 1 vol.%. It is worth noting here that the volume changes associated with the formation of the M₂AC phases from their elements is negative and ranges from 6 to 17 vol.% (Table 2).

Typical powder XRD spectra for the M₂SnC phases fabricated, at the times and temperature listed in Table 2, are plotted in Fig. 1. In all cases the main peaks belong to the ternary carbides. SEM and DSC analyses, however, indicated that the M₂SnC phases comprised 92–96 vol.% of the samples, with the Sn and MC_x phases making up the balance. A typical back-scattered SEM image of a Nb₂SnC sample is reproduced in Fig. 2. In this micrograph, the dark phase, is NbC_x, the volume fraction of which is determined by image analysis to be ~4 vol.%. The volume fractions of the other

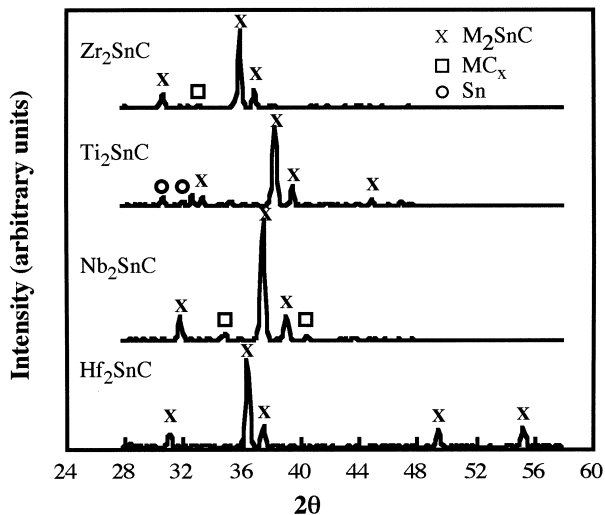


Fig. 1. Summary of XRD spectra for M_2SnC ternary phases.

MC_x phases are listed in Table 2. The corresponding volume fractions of Sn determined by DCS ranged from a low of 1 vol% for Hf_2SnC , to a high of 5.5 vol% for Ti_2SnC (Table 2).

A comparison of the XRD patterns of the M_2SnC phases obtained from this work and those in Ref. 10 reveals that the samples fabricated in this work have a higher content of the ternary carbides. The processing temperatures and times for Hf_2SnC and Nb_2SnC were identical to those used previously.¹⁰ However, for Ti_2SnC and Zr_2SnC longer processing times at lower temperatures [compared to Ref. 10], resulted in higher volume fractions of the M_2SnC phases. It is now believed that the previously reported processing temperatures for Ti_2SnC and Zr_2SnC were probably too close to their dissociation temperatures determined in this work to be 1250 and 1275°C, respectively.

3.2. Processing of M_2PbC compounds

The best Zr_2PbC samples were obtained by HIPing at 1200°C for 48 h, followed by annealing the same samples, without removing the encapsulating glass, at 1200°C for 96 h under Ar. A comparison of Fig. 3a and b, shows that the long anneal is necessary to fully react the unreacted Pb with the ZrC_x that forms during heat up of the samples. The Pb content, as determined from DSC measurements of the annealed samples, was <0.4 vol.%; the residual ZrC_x content was \approx 6 vol.%.

Samples of Hf_2PbC were fabricated by reactive HIPing at 1200°C for 48 h followed by annealing under Ar at 1200°C for 48 h. The XRD pattern of the annealed sample is shown in Fig. 3c. The final Pb content in the samples was estimated from the DSC to be \approx 2.5 vol.%; the HfC_x content was estimated to be \approx 2 vol.%.

Finally it is worth noting that despite the fact that the samples were found to contain less than 1 vol.%

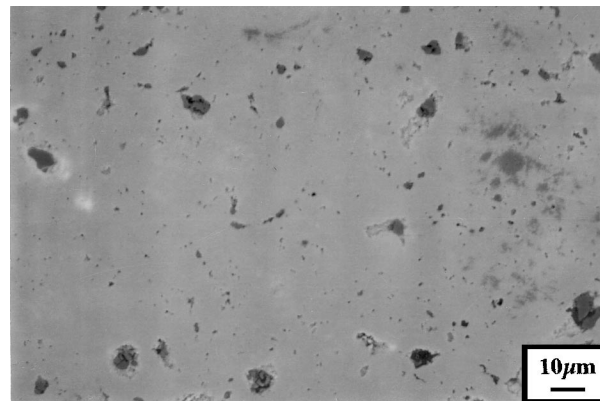


Fig. 2. SEM back scattered image of Nb_2SnC . Dark phase is NbC_x .

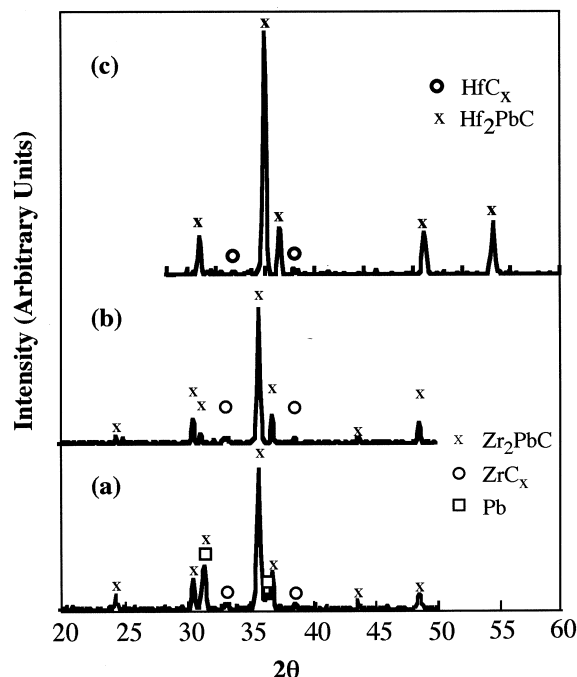


Fig. 3. XRD spectra a further M_2PbC phases. (a) Zr_2PbC after HIPing, (b) same as (a) but after 48 h anneal in Ar. Note reduction in binary carbide peaks, (c) Zr_2PbC after HIPing and annealing in Ar for 96 h.

porosity, their measured densities were either slightly lower than, in the case of the M_2SnC phases, or significantly lower than, in the case of the M_2PbC phases, the densities calculated based on the rule of mixtures (Table 2). This discrepancy can most probably be attributed to a combination of the following two reasons: (i) the reaction of the molten Sn or Pb with the encapsulating glass and its removal from the sample. Such a reaction has been documented and typically results in total dissociation of the ternaries in the vicinity of the glass into the MC_x ; (ii) the ternary compounds are substoichiometric in Sn or Pb; a possibility that has been suggested previously.^{1,2}

3.3. Characterization

The temperature dependencies of the thermal expansions of the ternary carbides upon heating and cooling are plotted in Fig. 4a. (The curves are shifted by 300°C to the right for clarity.) A least squares fit of the data yields the values of the TCE's listed in Table 3.² Also listed in Table 3 are the corresponding TCE's of the stoichiometric binaries. Fig. 4b plots the TCE's of both the binary and ternary compounds as a function of the melting point of the stoichiometric binary carbides. The implications of these results are several. First, the M–A bonds are clearly weaker than the M–C bonds, but significantly stronger than the A–A bonds. Second, the Pb–M and Sn–M bonds are more or less comparable.

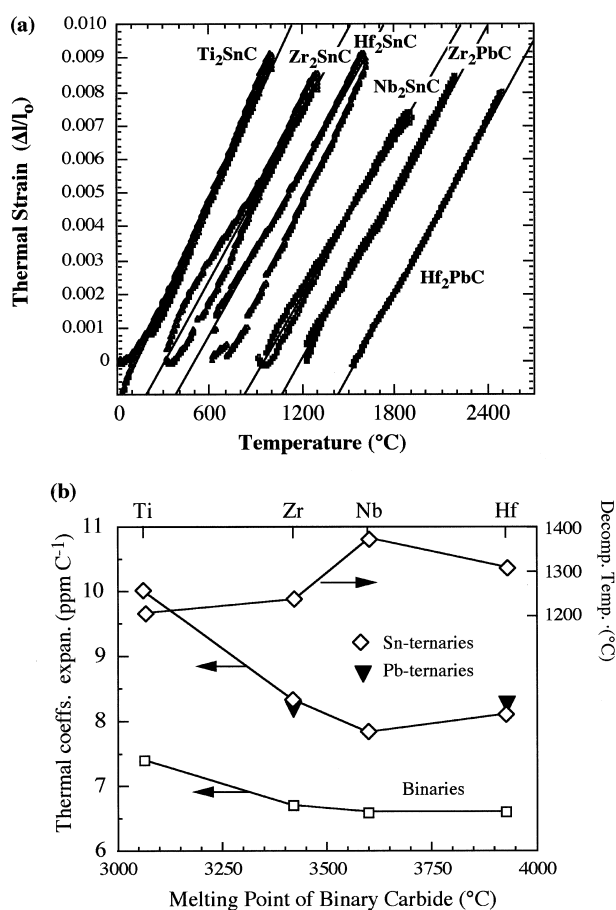


Fig. 4. (a) Temperature dependence of thermal expansions of M_2AC phases upon heating and cooling. Least squares fits of the results are shown by lines superimposed on the data. For the Hf-containing samples the TCE's were calculated from the cooling curves. (b) Comparison of TCE's of M_2AC phases and those of the corresponding stoichiometric binary carbides, MC versus the melting point of the latter. Top curve plots decomposition temperature of M_2SnC phases.

² For the Hf-containing ternaries there was marked hysteresis upon heating and cooling. In that case, the least squares fit was constrained to the cooling curves which are deemed more accurate because the effect of oxidation or other potential reactions are minimized.

Third, the TCE of the ternaries correlate well with those of the corresponding stoichiometric binaries, with the latter being 20–33% higher. This in turn implies that the M–C bonds in the ternary compounds are comparable to their counterparts in the stoichiometric binary compounds. It is also probable that some of the M–C bonds in the ternaries are even stronger as is the case for Ti_3SiC_2 and Ti_4AlN_3 .^{12,22}

For reasons that are not clear the TCE of Hf_2SnC is slightly higher than one would have anticipated from Fig. 4b. This result, however, is consistent with the independent fact that the dissociation temperature of Hf_2SnC is slightly lower (i.e. less stable) than that of Nb_2SnC (Fig. 4b, right hand side).

The Young's moduli of the compounds measured range from 178 GPa for Zr_2SnC to 237 GPa for Hf_2SnC , with that of Nb_2SnC , at 216 GPa, in between. These values are about 50% lower than the corresponding stoichiometric binary carbides, once again, reflecting the weakness of the M–Sn bonds relative to the M–C bonds. Unfortunately, it was difficult to fabricate Ti_2SnC or the Pb-containing specimens of adequate geometry to obtain reliable pulse echo measurements.

The Vickers hardness values were found to be independent of load. Within the scatter in the results listed in Table 3, the hardness values appear to be insensitive to the composition and range from a low of 3.2 to a high of 3.9 GPa. The values are consistent with the Vickers hardness values of most other M_2AC phases,^{8,9} including the M_2SnC phases.¹⁰ All the compounds possessed excellent machinability. They can be machined by a manual hack-saw, milling machine, or lathe with regular tool bits; no lubrication or cooling is required.

The resistivities of the compounds fabricated in this work are plotted versus temperature in Fig. 5. The electric conductivities of the ternary compounds are quite high; they range from a low of 2.2×10^6 ($\Omega \cdot m$)⁻¹ for Hf_2SnC , to a high of 13.4×10^6 ($\Omega \cdot m$)⁻¹ for Hf_2PbC , with the others falling in between (Table 3). The conductivity of Hf_2PbC is noteworthy, not only because it is quite high ($\approx 1/3$ of Al metal), but also because it is significantly higher than either pure Pb or HfC (Table 3). The α 's range from a low of 0.0021 for Nb_2SnC , to a high of 0.0144 for Hf_2PbC . Comparing the results measured in this work and those previously reported¹⁰ it is clear that with the exception of the Hf_2SnC , the reproducibility is rather poor. This implies that there is a hidden variable influencing the conductivity results. At this time, it is not clear what that variable is, but it could be related to small differences in the stoichiometry of the ternary carbides or the presence of small concentrations of impurities introduced either with the starting powders or during processing.

Finally it is worth noting that the Pb-containing ternaries are not stable, but are slowly attacked upon exposure to the atmosphere. Fig. 6 is a SEM secondary

Table 3

Comparison of physical properties M_2AC carbides measured in this work and the corresponding values for the stoichiometric binary carbides. Also included are the results of our previous work¹⁰

	Estimated dissociation temperature or melting point (°C)	Thermal coefficient of expansion (ppm/K)	R.T. electrical resistivity (ρ) ($\mu\Omega\cdot m$)	Temperature coefficient of resistivity (α) (K^{-1})	Elastic modulus (GPa)	Vickers hardness (GPa)
Ti_2SnC	1250	10 ± 0.2	0.22 0.07 ¹⁰	0.0032 0.0040 ¹⁰	— ^a	3.5 ± 0.4 3.5 ± 0.4^{10}
Zr_2SnC	1275	8.3 ± 0.2	0.28 0.14 ¹⁰	0.0035 0.004 ¹⁰	178	3.9 ± 0.3 3.5 ± 0.4^{10}
Nb_2SnC	1390 ± 25^{10}	7.8 ± 0.2	0.45 0.25 ¹⁰	0.0021 0.009 ¹⁰	216	3.8 ± 0.2 3.5 ± 0.4
Hf_2SnC	1335 ± 25^{10}	8.1 ± 0.2	0.45 0.42 ¹⁰	0.0034 0.0027 ¹⁰	237	3.8 ± 0.7 4.5 ± 0.4^{10}
Zr_2PbC	< 1300	8.2 ± 0.2	0.36	0.0144	— ^a	3.2 ± 0.5
Hf_2PbC	< 1300	8.3 ± 0.2	0.075	0.0063	— ^a	3.8 ± 0.7
Ti_3SiC_2	≈ 2200 ²³	9.2	0.22	0.004 ¹⁰	330 ^{21,24}	4
TiC ²⁵	3067 (mp)	7.4	0.4–0.59		410–510	28–35
ZrC ²⁵	3420 (mp)	6.7	0.34–0.56		350–440	25.5
NbC ²⁵	3600 (mp)	6.6	0.56		338–580	19.65
HfC ²⁵	3928 (mp)	6.6	0.45–0.37		350–510	26.1
Sn	232 (mp)	19.9	0.1	0.0047	39–54	
Pb	327 (mp)	29.3	0.2	0.0034	14–17	

^a Not measured.

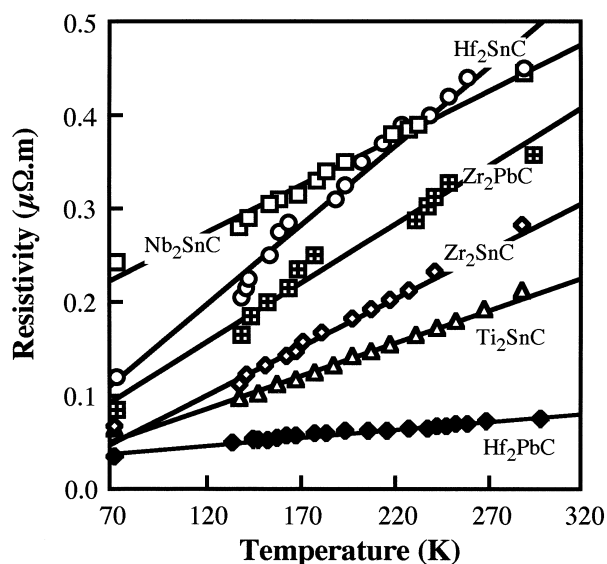


Fig. 5. Temperature dependence of resistivities of M_2AC phases fabricated in this work.

image of a polished sample of Hf_2PbC that had been exposed to the atmosphere for 24 h. The salient features are the protrusions and cracks formed as a result of atmospheric attack. The volume expansion is so severe that a few days exposure to the atmosphere results in the cracking of the mounting material and the disintegration of the sample into a powder heap. Interestingly enough, at the resolution level of XRD, there were no discernable differences in the spectra of the bulk, unreacted material and the resulting powders. The nature of the attack is thus not understood, but is most

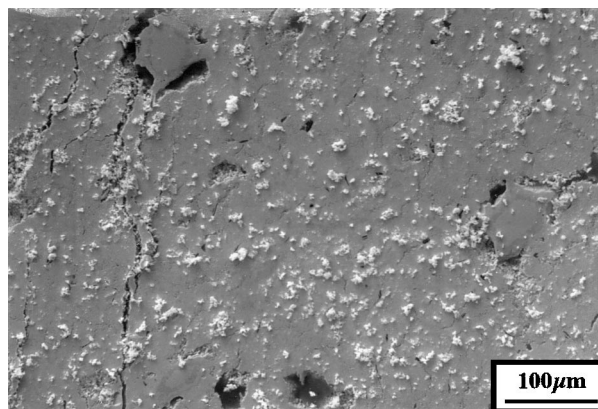


Fig. 6. SEM secondary image of Hf_2PbC that had been exposed to the atmosphere for 24 h.

likely an oxidative process. Consistent with these observations are the results of the oxidation of Hf_2SnC and Nb_2SnC in the 400–600°C temperature range.²⁰ The oxidation kinetics are linear and are associated with a large volume expansion that also results in the total disintegration of the ternaries into a pile of powder of the corresponding transition metal oxide (HfO_2 or Nb_2O_5) and SnO at lower temperatures, and/or SnO_2 at higher temperatures.

4. Conclusions:

- Predominantly single phase (92–94%), fully dense samples of Hf_2SnC and Zr_2SnC , Nb_2SnC , Hf_2SnC , Hf_2PbC and Zr_2PbC phases were fabricated by

reactively HIPing the stoichiometric mix of the corresponding elemental powders in the 1200–1325°C temperature range. The Pb-containing ternaries were fabricated for the first time and found to be unstable in ambient atmospheres at room temperature.

- The TCE's of the M_2AC phases scale with those of the corresponding *stoichiometric* transition metal binary carbides or MC. The TCE's are thus quite low for such readily machinable solids; the lowest ($7.8 \times 10^{-6} \text{ K}^{-1}$) is that of Nb_2SnC , and the highest ($10 \times 10^{-6} \text{ K}^{-1}$) belongs to Ti_2SnC . The TCE's of Hf and Zr containing ternaries cluster around $(8.2 \pm 0.2) \times 10^{-6} \text{ K}^{-1}$. The TCE's of the Pb-containing ternaries were almost identical to those of the corresponding Sn-containing ones.
- The ternaries are good electrical conductors, with conductivities in the $2\text{--}14 \times 10^6 (\Omega\text{-m})^{-1}$ range. The temperature coefficients of resistivity range from 0.002 to 0.015 K^{-1} .
- The Young's moduli Zr_2SnC , Nb_2SnC and Hf_2SnC are, respectively, 178, 216 and 237 GPa. The Vickers hardness values vary from 3 to 4 GPa.

Acknowledgements

We would like to thank Mr. P. Finkel of Physical Acoustics, Corp., Princeton, NJ, for carrying out the ultrasonic measurements. This work was supported by the DMR division of NSF (DMR-9705237).

References

1. Jeitschko, W., Nowotny, H. and Benesovsky, F., Die H-phasen Ti_2TiC , Ti_2PbC , Nb_2InC , Nb_2SnC und Ta_2GaC . *Monatsh. Chem.*, 1964, **95**, 431.
2. Jeitschko, W., Nowotny, H. and Benesovsky, F., Kohlenstoffhaltige ternäre Verbindungen (H-Phase). *Monatsh. Chem.*, 1963, **94**, 672.
3. Jeitschko, W. and Nowotny, H., Die Kristallstruktur von Ti_3SiC_2 -Ein Neuer Komplexcarbid-Typ. *Monatsh. Chem.*, 1967, **98**, 329–337.
4. Pietzka, M. and Schuster, J. C. The ternary boundary phases of the quaternary system Ti–Al–C–N. In *Concerted Action on Materials Science, Leuven Proceedings, Part A*. Commission of the European Communities, Brussels, Belgium, 1992.
5. Barsoum, M. W., Farber, L., Levin, I., Procopio, A., El-Raghy, T. and Berner, A., HRTEM of Ti_4AlN_3 ; or $Ti_3Al_2N_2$ Revisited. *J. Am. Ceram. Soc.*, 1999, **82**, 2545–2547.
6. Rawn, C. J., Barsoum, M. W., El-Raghy, T., Procopio, A., Hoffmann, C. M. and Hubbard, C. Structure of Ti_4AlN_{3-x} — a layered $M_{n+1}AX_n$ nitride. *Mater. Res. Bulletin*, in press.
7. Barsoum, M. W. and El-Raghy, T., Synthesis and characterization of a remarkable ceramic: Ti_3SiC_2 . *J. Am. Ceram. Soc.*, 1996, **79**, 1953–1956.
8. Barsoum, M. W., Brodtkin, D. and El-Raghy, T., Layered machinable ceramics for high temperature applications. *Scrip. Met. Mater.*, 1997, **36**, 535–541.
9. Barsoum, M. W. and El-Raghy, T., A Progress report on Ti_3SiC_2 , Ti_3GeC_2 and the H-phases, M_2BX . *J. Mater. Synth. Process.*, 1997, **5**, 197–216.
10. Barsoum, M. W., Yaroshuck, G. and Tyagi, S., Fabrication and characterization of M_2SnC ($M=Ti, Zr, Hf$ and Nb). *Scrip. Mater.*, 1997, **37**, 1583–1591.
11. Low, I. M., Lee, S. K., Lawn, B. and Barsoum, M. W., Contact damage accumulation in Ti_3SiC_2 . *J. Am. Ceram. Soc.*, 1998, **81**, 225–228.
12. Barsoum, M. W., El-Raghy, T., Rawn, C. J., Porter, W. D., Payzant, A. and Hubbard, C., Thermal properties of Ti_3SiC_2 . *J. Phys. Chem. Solids*, 1999, **60**, 429–439.
13. Procopio, A., Barsoum, M. W. and El-Raghy, T., Characterization of Ti_4AlN_3 . *Met. Mat. Trans.*, 2000, **31A**(2), 333–337.
14. Tzenov, N. and Barsoum, M. W., Synthesis and characterization of $Ti_3AlC_{1.8}$. *J. Am. Ceram. Soc.*, 2000, **83**, 825–832.
15. Farber, L., Barsoum, M. W., Zavaliangos, A., El-Raghy, T. and Levin, I., Dislocations and stacking faults in Ti_3SiC_2 . *J. Am. Ceram. Soc.*, 1998, **81**, 1677–1681.
16. Barsoum, M. W. and El-Raghy, T., Room temperature ductile carbides. *Met. Mat. Trans.*, 1999, **30A**, 363–369.
17. Barsoum, M. W., Farber, L., El-Raghy, T. and Levin, I., Dislocations, kink banks and room temperature plasticity of Ti_3SiC_2 . *Met. Mat. Trans.*, 1999, **30A**, 1727–1738.
18. El-Raghy, T., Barsoum, M. W., Zavaliangos, A. and Kalidindi, S., Processing and mechanical properties of Ti_3SiC_2 , part II: mechanical properties. *J. Am. Ceram. Soc.*, 1999, **82**, 2855–2859.
19. Radovic, M., Barsoum, M. W., El-Raghy, T., Seidensticker, J. and Wiederhorn, S., Tensile properties of Ti_3SiC_2 in the 25–1300°C temperature range. *Acta. Mater.*, 2000, **48**, 453–459.
20. Chakraborty, S. MSc thesis, Drexel University, June 1998.
21. Finkel, P., Barsoum, M. W. and El-Raghy, T., Low temperature dependence of elastic properties of Ti_3SiC_2 . *J. Appl. Phys.*, 1999, **85**, 7123–7126.
22. Barsoum, M. W., Rawn, C. J., El-Raghy, T., Procopio, A., Porter, W. D., Wang, H. and Hubbard, C. R. Thermal properties of Ti_4AlN_3 . *J. Appl. Phys.*, 2000, **87**, 8407–8414.
23. Du, Y., Schuster, J. C., Seifert, H., and Aldinger, F. *J. Am. Ceram. Soc.*, 2000, **83**, 197–203.
24. Pampuch, R., Lis, J., Stobierski, L. and Tymkiewicz, M. Solid combustion synthesis of Ti_3SiC_2 . *J. Eur. Ceram. Soc.*, 1989, **5**, 283.
25. Pierson, H., *Handbook of Refractory Carbides and Nitrides*. Noyes Pubs, Westwood, NJ, 1996.